

NUMERICAL SIMULATION OF THERMOCHEMICAL NONEQUILIBRIUM HYPERSONIC FLOWS USING THE TAYLOR-GALERKIN SCHEME

Martin P. Kessler

PROMECA, Universidade Federal do Rio Grande do Sul. Rua Sarmento Leite, 425, 3 andar, 90050-170, Porto Alegre, RS, Brazil.
kessler@ig.com.br

Armando M. Awruch

PPGEC, Universidade Federal do Rio Grande do Sul. Av. Osvaldo Aranha, 99, 3 andar, 90035-190, Porto Alegre, RS, Brazil.
awruch@adufgrs.ufrgs.br

Abstract. The aim of the present work is to introduce a formulation for the numerical analysis of three-dimensional thermochemical nonequilibrium hypersonic flows, using the finite element method and the Taylor-Galerkin scheme and adopting Park's 2-temperature, 5-species (N_2 , O_2 , NO , N and O) and 17-reaction model. Special interest of the work is in analyzing the reentry of the Atmospheric Reentry Satellite (SARA), a non-manned recoverable orbital system developed by the National Space Research Institute (INPE) and by the Aerospace Technical Center (CTA) to offer a return-on-request concept in order to perform micro-gravity experiments.

Keywords. Hypersonic flow, thermochemical nonequilibrium, reentry aerodynamics, numerical simulation, finite elements.

1. Introduction

Reentering the Earth's atmosphere is a phenomenon that has challenged researchers over the last decades. Due to the growth of space exploration and the increasing number of space trips, great interest in dominating launch, orbit and recovery of space vehicles has been created, primarily to bring back people and experiments safely to Earth.

Since the beginning of the Space Age, marked by the Sputnik launch in October 4th, 1957, great interest in operating recoverable space vehicles is being created by researchers and scientists. The recovery of a space vehicle is a very complex procedure, including its reentry into the Earth's atmosphere at large speeds, usually reaching the hypersonic regime ($Mach > 5$). For an orbital vehicle, reentry starts at $Mach = 25$ approximately (around 8 km/s), and for a vehicle returning from the Moon, as performed by Apollo, reentry starts at $Mach = 36$ approximately (around 11 km/s). Due to these high speeds, extremely high temperatures are generated around the vehicle, which may cause vibrational excitation, dissociation and ionization of the molecules. Therefore, the perfect gas hypothesis is no longer valid for air at those regimes and one must include high temperature effects in the mathematical model to properly analyze hypersonic flows.

For high temperature analysis, knowledge of thermodynamic gas properties is needed. Some of those properties cannot be obtained from classic thermodynamics. On the other hand, statistic thermodynamics allows scientists to obtain those properties from basic principles. For a simple diatomic molecule ("dumbbell" model), the internal energy can be split in four modes: translational, rotational, vibrational and electronic (Anderson, 1989). Above specific temperatures (around 800 K for air at 1 atm), the molecules become vibrationally excited and the modes can no longer be represented by one single temperature (thermal nonequilibrium).

For high temperature hypersonic flows with chemical reactions, the vibrational temperature is very important, because it controls the molecular dissociation rate (Brown, 1986). Park (1990) suggests that without taking into account the vibrational temperature, there is a little chance that a CFD analysis be able to reproduce the experimentally observed phenomena. Lee (1985) presented a basic formulation for flight analysis of Aeroassisted Orbital Transfer Vehicles (AOTV), which includes three energy conservation equations: total, vibrational and electronic. Park (1985) introduced a simpler version, with only two energy conservation equations (total and vibrational), where vibrational and electronic temperature, T_v , are considered to be in equilibrium, but independent of the translational-rotational temperature, T .

Supersonic flow around a blunt body were first solved numerically by Moretti & Abbett (1966). They employed a time-marching finite difference technique, developed by Lax & Wendroff (1960, 1962, 1964), applied to the transient Euler equations. Computer codes including physical phenomena present in hypersonic flows appeared in the early 1970's (Désidéri, 1991). In the context of the finite element method (FEM), Donea (1984) developed a time-marching procedure, the Taylor-Galerkin scheme, which is considered the equivalent of Lax-Wendroff method for FEM (Codina, 1998; Saffjan & Oden, 1995). Argyris *et al.* (1989, 1990, 1991, 1994) applied the Taylor-Galerkin scheme to analyze the reentry of the European space vehicle, Hermes, into the Earth's atmosphere. They used a hypersonic mathematical model with chemical reactions and thermal equilibrium (one temperature).

The aim of the present work is to introduce a procedure to solve thermochemical nonequilibrium hypersonic flows using the Taylor-Galerkin scheme and Park's two-temperature model. Ionization is neglected, and only 5 chemical species are considered (N_2 , O_2 , NO , N and O). Three non diffusive examples are presented: the hypersonic flow of

partially dissociated nitrogen over a cylinder, the hypersonic flow over a half-ellipse and the hypersonic flow over the SARA vehicle.

2. The mathematical model

2.1 Governing equations

A formulation for non diffusive thermochemical nonequilibrium hypersonic flows is presented. Einstein notation is used, so summation along repeated indexes occur unless otherwise indicated. Subscript s refers to the species. Five different types of conservation equations are applied: mass of the mixture, mass for each species, momentum, vibrational and total energies. They are gathered in a compact form, as follows:

$$\frac{\partial U}{\partial t} + \frac{\partial F_j}{\partial x_j} + H = 0 \quad (1)$$

where

$$U = \begin{Bmatrix} \rho \\ \rho_s \\ \rho u_i \\ \rho e_v \\ \rho e \end{Bmatrix}, \quad F_j = \begin{Bmatrix} \rho u_j \\ \rho_s u_j \\ \rho u_i u_j + p \delta_{ij} \\ \rho e_v u_j \\ (\rho e + p) u_j \end{Bmatrix}, \quad H = \begin{Bmatrix} 0 \\ -\omega_s \\ 0 \\ -\omega_v \\ 0 \end{Bmatrix} \quad (2)$$

where ρ is the specific mass of the mixture, ρ_s is the specific mass of the species s , u_i is the velocity component in x_i direction, δ_{ij} is the Kronecker delta, ω_s and ω_v are the mass and vibrational/electronic energy sources, respectively. The pressure, p , is obtained from Dalton's Law of Partial Pressures, as follows:

$$p = \sum_{s=1}^{N_s} p_s = \sum_{s=1}^{N_s} \rho_s R_s T \quad (3)$$

where p_s and R_s are the partial pressure and the gas constant for species s , respectively, T is the translational temperature and N_s is the number of species. The vibrational energy, e_v , and the total energy, e , are defined by

$$e_v = c_s e_{v,s} \quad (4)$$

$$e = \frac{1}{2} u_j u_j + c_s (e_{t,s} + e_{v,s} + e_{o,s})$$

with

$$e_{t,s} = \begin{cases} \frac{3}{2} R_s T, & s = \text{atom} \\ \frac{5}{2} R_s T, & s = \text{molecule} \end{cases} \quad (5)$$

$$e_{v,s} = \begin{cases} 0, & s = \text{atom} \\ \frac{R_s \theta_{v,s}}{\exp(\theta_{v,s} / T_v) - 1}, & s = \text{molecule} \end{cases} \quad (6)$$

where c_s is the mass fraction, T_v is the vibrational temperature, $e_{t,s}$ and $e_{v,s}$ are the translational and vibrational internal energies, respectively, $e_{o,s}$ is the formation energy and $\theta_{v,s}$ is the vibrational characteristic temperature. The data for each of the 5 species are given in Tab. (1).

Table 1 – Data for the 5 species.

	N ₂	O ₂	NO	N	O
M _s [kg/kg-mole]	28.02	32.00	30.01	14.01	16.00
R _s [J/kg K]	296.7	259.8	277.04	593.6	519.6
e _{o,s} [J/kg]	0	0	2.99×10 ⁶	33.59×10 ⁶	15.42×10 ⁶
θ _{v,s} [K]	3393	2270	2740	-	-

2.2 Source Terms

The vibrational/electronic energy source is given by (Gnoffo, 1989):

$$\omega_v = \rho_s \frac{e_{v,s}(T) - e_{v,s}(T_v)}{\tau_s} + [e_{v,s}(T_v) + e_{e,s}(T_v)]\omega_s \quad (7)$$

where

$$\tau_s = \left(\sum_{r=1}^{N_s} \frac{y_r}{\tau_{sr}} \right)^{-1} \quad (8)$$

$$\tau_{sr} = \frac{\exp[A_{sr}(T^{-1/3} - 0.015B_{sr}^{1/4}) - 18.42]}{p} \quad (9)$$

$$A_{sr} = 1.16 \times 10^{-3} B_{sr}^{0.5} \theta_{v,s}^{4/3}, \quad B_{sr} = \frac{M_s M_r}{M_s + M_r} \quad (10)$$

where y_s is the molar fraction and M_s is the molecular weight. The pressure, p , in Eq. (9) must be inserted in atmospheres to obtain relaxation time in seconds.

The mass rate of production of species s is given by (Gnoffo, 1989):

$$\omega_s = M_s \sum_{r=1}^{N_r} (b_{s,r} - f_{s,r}) (R_{f,r} - R_{b,r}), \quad (\text{no summation on } s) \quad (11)$$

where N_r is the number of reactions, $f_{s,r}$ and $b_{s,r}$ are respectively the stoichiometric coefficients for reactants and products in the r reaction, $R_{f,r}$ and $R_{b,r}$ are respectively the forward and backward reaction rates for r reaction. These rates are defined by:

$$R_{f,r} = k_{f,r} \prod_{s=1}^{N_s} \left(\frac{\rho_s}{M_s} \right)^{f_{s,r}}, \quad R_{b,r} = k_{b,r} \prod_{s=1}^{N_s} \left(\frac{\rho_s}{M_s} \right)^{b_{s,r}} \quad (12)$$

where $k_{f,r}$ and $k_{b,r}$ are the forward and backward reaction rate coefficients, respectively, given by:

$$k_{f,r} = C_{f,r} T_x^{n_{f,r}} \exp(-T_d / T_x)$$

$$k_{b,r} = \frac{k_{f,r}}{K_{eq,r}}, \quad (\text{no summation on } s) \quad (13)$$

$$K_{eq,r} = \exp(B_{1,r} + B_{2,r} \ln Z + B_{3,r} Z + B_{4,r} Z^2 + B_{5,r} Z^3)$$

where

$$Z = \frac{10^4}{T} \quad (14)$$

The parameters $C_{f,r}$, $n_{f,r}$, T_d , T_x , $B_{1,r}$, $B_{2,r}$, $B_{3,r}$, $B_{4,r}$ and $B_{5,r}$, are those defined by Park (1986). The dissociation reactions are controlled by a combination of the two temperatures, as proposed by Park (1986), as follows:

$$T_a = \sqrt{TT_v} \quad (15)$$

3. The Finite Element Taylor-Galerkin Scheme

3.1 Time discretization: Taylor Series

In Taylor-Galerkin scheme, the variables are expanded in time according to a Taylor Series, as follows (Yoon *et al.*, 1998):

$$U^{n+1} = U^n + \Delta t \left(\frac{\partial U}{\partial t} \right)^{n+s_1} + \frac{\Delta t^2}{2} \left(\frac{\partial^2 U}{\partial t^2} \right)^{n+s_2} + O(\Delta t^3) \quad (16)$$

where the superscript identifies the time step. Thus, one can obtain the results in time step $n+1$ with information from the previous step, n . In addition, the following definitions are given:

$$\begin{aligned} \frac{\partial U^{n+s_1}}{\partial t} &= \frac{\partial U^n}{\partial t} + s_1 \frac{\partial \Delta U^{n+1}}{\partial t} & 0 \leq s_1 \leq 1 \\ \frac{\partial^2 U^{n+s_2}}{\partial t^2} &= \frac{\partial^2 U^n}{\partial t^2} + s_2 \frac{\partial^2 \Delta U^{n+1}}{\partial t^2} & 0 \leq s_2 \leq 1 \end{aligned} \quad (17)$$

Adopting $s_1 = s_2 = 1/2$ and substituting in (16), one obtains:

$$\Delta U^{n+1} = \Delta t \left(\frac{\partial U^n}{\partial t} + \frac{1}{2} \frac{\partial \Delta U^{n+1}}{\partial t} \right) + \frac{\Delta t^2}{2} \left(\frac{\partial^2 U^n}{\partial t^2} + \frac{1}{2} \frac{\partial^2 \Delta U^{n+1}}{\partial t^2} \right) \quad (18)$$

where $\Delta U^{n+1} = U^{n+1} - U^n$. From Eq. (1), the time derivative for U^n is defined as:

$$\frac{\partial U^n}{\partial t} = -\frac{\partial F_j^n}{\partial x_j} - H^n \quad (19)$$

Similarly, the time derivative for ΔU^{n+1} is defined as:

$$\frac{\partial \Delta U^{n+1}}{\partial t} = -\frac{\partial \Delta F_j^{n+1}}{\partial x_j} - \Delta H^{n+1} \quad (20)$$

Substituting Eqs. (19) and (20) in Eq. (18), neglecting all terms greater than second order and introducing an iteration counter for the incremental terms, the following expression is obtained:

$$\Delta U_{i+1}^{n+1} = \Delta t \left[-\frac{\partial F_j^n}{\partial x_j} - H^n + \frac{\Delta t}{2} \frac{\partial}{\partial x_j} \left(u_j^n \frac{\partial F_k^n}{\partial x_k} \right) \right] + \frac{\Delta t}{2} \left[-\frac{\partial \Delta F_j^{n+1}}{\partial x_j} + \frac{\Delta t}{2} \frac{\partial}{\partial x_j} \left(u_j^n \frac{\partial \Delta F_k^{n+1}}{\partial x_k} \right) \right] \quad (21)$$

Here a fixed time-step was adopted and it satisfies the CFL condition, i. e. $\Delta t \leq \alpha \Delta x / (u + c)$ (where Δx is a characteristic dimension of the element with the minimum volume, $\alpha < 1.0$ is a safety coefficient and c is the speed of sound). Steady state is reached when the relative values of the variables between two successive time steps are less than a given tolerance.

3.2 Spatial discretization: Galerkin weighted residual method

Spatial discretization of Eq. (21) is obtained through application of the classical Galerkin method. The variables are evaluated in each node of the element, as follows:

$$U^n = [\Phi]\{U\}^n \quad (22)$$

where $[\Phi]$ is the line matrix of the shape functions and $\{U\}^n$ is the nodal values of the variable. Eight-node three dimensional hexahedron isoparametric elements are used in this work, whose shape functions are given by

$$\Phi_N = \frac{1}{8} [1 + \xi_{1N} \xi_1] [1 + \xi_{2N} \xi_2] [1 + \xi_{3N} \xi_3] \quad (23)$$

where N is the local node number (1 to 8), ξ_{1N} , ξ_{2N} and ξ_{3N} are the natural coordinates of local node N .

Substituting Eq. (22) in Eq. (21) and applying the weighted residual method, one obtains

$$\{\Delta U\}_{I+1}^{n+1} = \Delta t [M_L]^{-1} \left\{ -[A_i]\{F_i\}^n - [M]\{H\}^n + \frac{\Delta t}{2}\{f\}^n \right\} + \frac{\Delta t}{2} [M_L]^{-1} \left\{ -[A_i]\{\Delta F_i\}_I^{n+1} \right\} \quad (24)$$

where $\{\Delta U\}_{I+1}^{n+1}$ is the incremental value of the variables evaluated in step time $n+1$ and iteration $I+1$ for each element node, $[M]$ and $[M_L]$ are the mass and lumped mass matrices, respectively, $[A_i]$ is the matrix for advection, $\{F_i\}^n$, $\{H\}^n$ and $\{\Delta F_i\}_I^{n+1}$ are the nodal values for advection, source and incremental advection, respectively, $\{f\}^n$ is the boundary nodal values for advection. These definitions are fully described in Kessler (2002). Once the incremental value is calculated, the variables are updated as follows:

$$\{U\}^{n+1} = \{U\}^n + \{\Delta U\}^{n+1} \quad (25)$$

4. Numerical Results

4.1 Nitrogen flow over a half-cylinder

The non-diffusive hypersonic flow of nitrogen partially dissociated over a half-cylinder with 25.4 mm radius is analyzed. The free flow conditions are Mach = 6.13, temperature = 1833 K, velocity = 5590 m/s, density = 5.349×10^{-3} kg/m³ and atomic nitrogen mass fraction = 0.073. This problem was analyzed experimentally by Hornung (1972) and numerically by Ait-Ali-Yahia & Habashi (1997). The five-species model is employed, but three species (O₂, NO and O) are neglected in order to perform this 2-species problem (N₂ and N).

Due to symmetry, only the upper half of the cylinder is analyzed. Since this is a two-dimensional problem, but the code solves 3D problems, only one element is used in the x_3 direction ($\Delta x_3 = 0.005$ m). The finite element mesh is constituted of 1500 elements (50x30x1 elements) with 3162 nodes and is shown in Fig. (1a).

The Mach number contours are shown in Fig (1b). In Figs. (2a) and (2b) the temperatures and mass fraction distributions along stagnation line, respectively, are shown. The numerical shock position obtained by the present work agrees with the experimental shock position obtained by Hornung (1972), as can be seen in Fig. (2a). The result for perfect gas model fails to find the correct position of the shock. Furthermore, the temperature for perfect gas model remains practically unchanged between the shock and the cylinder's surface, while for the model with high temperature effects, the temperatures distributions have a maximum peak just after the shock and they continuously decrease towards the cylinder surface. This effect is explained by the chemical reactions, since dissociation is endothermic. In Fig. (2b), it can be seen that the mass fraction distributions along the stagnation line are less steep than the temperature ones. This phenomenon was expected, since chemical reactions need a large number of collisions to occur.

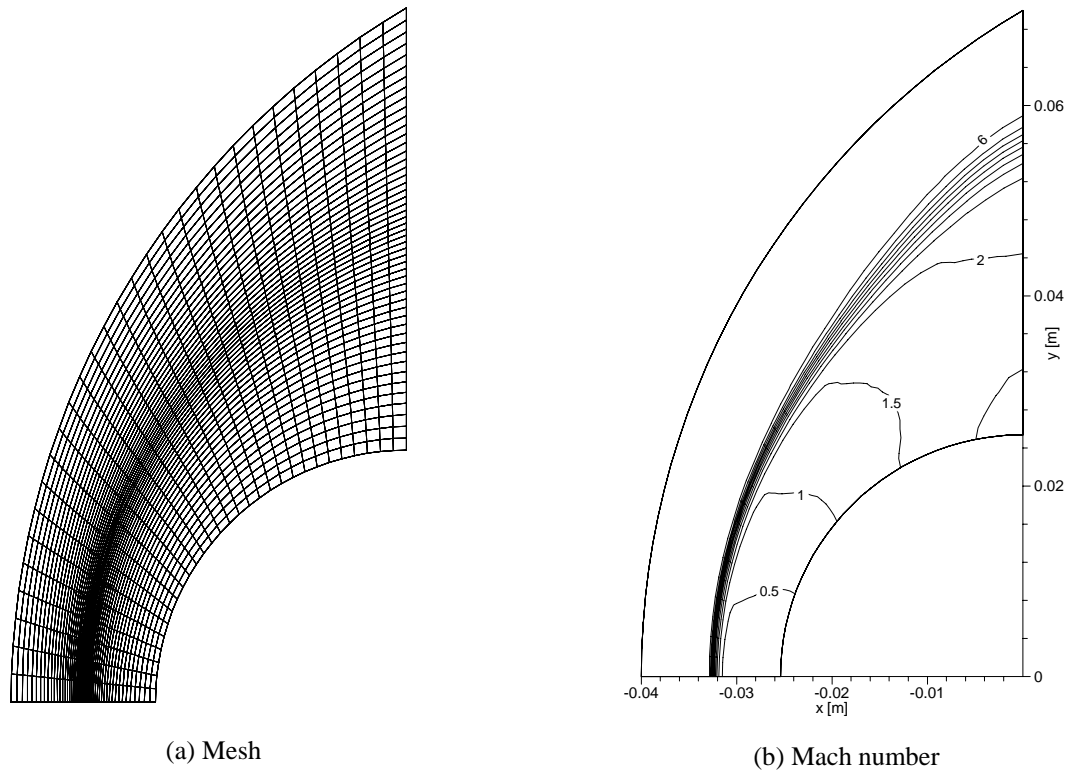


Figure 1. Finite element mesh (a) and Mach number contours (b).

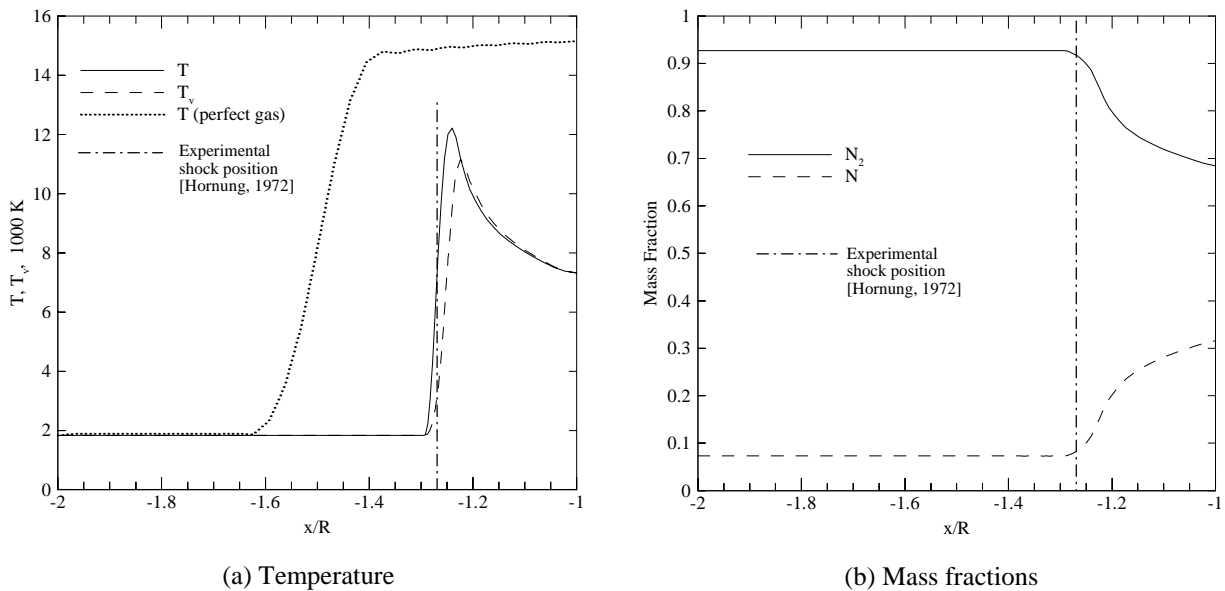


Figure 2. Temperature (a) and mass fractions (b) distributions along the stagnation line.

4.2 Hypersonic flow of air around a half-ellipse

Non-diffusive hypersonic flow of air in thermal equilibrium around a half-ellipse travelling at an altitude of 75 km is analyzed. The semi-axis of the ellipse are $a = 6.0$ cm and $b = 1.5$ cm. The free stream conditions are: Mach number = 25, velocity = 7250 m/s, temperature = 208.399 K, pressure = 2.388 Pa, density = 3.991×10^{-5} kg/m³, mass fraction of molecular nitrogen = 0.767, mass fraction of molecular oxygen = 0.233, mass fraction of the other 3 species = 0. This problem was analyzed by Argyris *et al.* (1989, 1991).

Due to symmetry, only the upper half of the ellipse is analyzed. Since this is also a two-dimensional problem, only one element is used in x_3 direction ($\Delta x_3 = 0.005$ m). The finite element mesh is constituted of 3600 elements ($60 \times 60 \times 1$ elements) with 7442 nodes and is shown in Fig. (3).

In Figs. (4a) and (4b) are shown the Mach number and the temperature contours, respectively. Figures (5a), (5b), (6a) and (6b) show the results obtained in the present work and those obtained by Argyris *et al.* (1989, 1991) for temperature, pressure, mixture density and mass fractions distributions along stagnation line, respectively. It can be seen that the results of this work are in good agreement with those of Argyris *et al.* (1989, 1991).

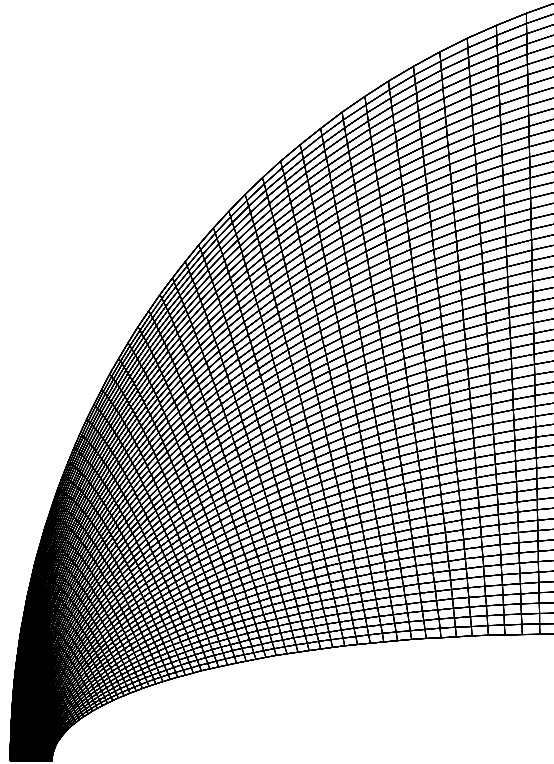
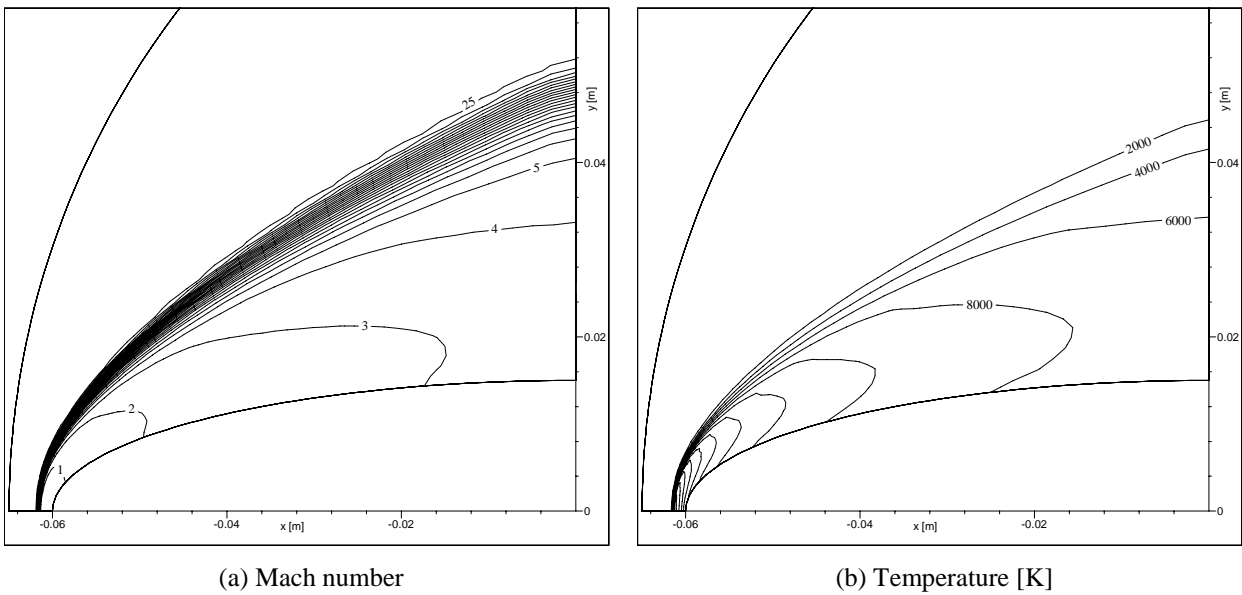


Fig. 3 – Finite element mesh for the ellipse problem.



(a) Mach number

(b) Temperature [K]

Figure 4. Mach number (a) and temperature (b) contours.

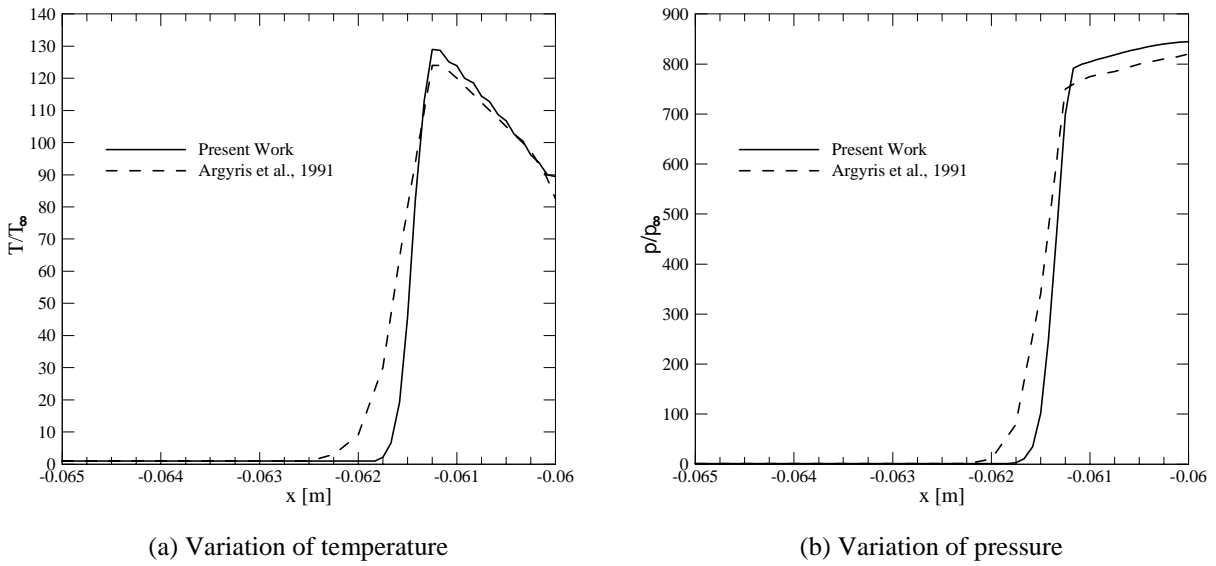


Figure 5. Variation of temperature (a) and of pressure (b) along the stagnation line.

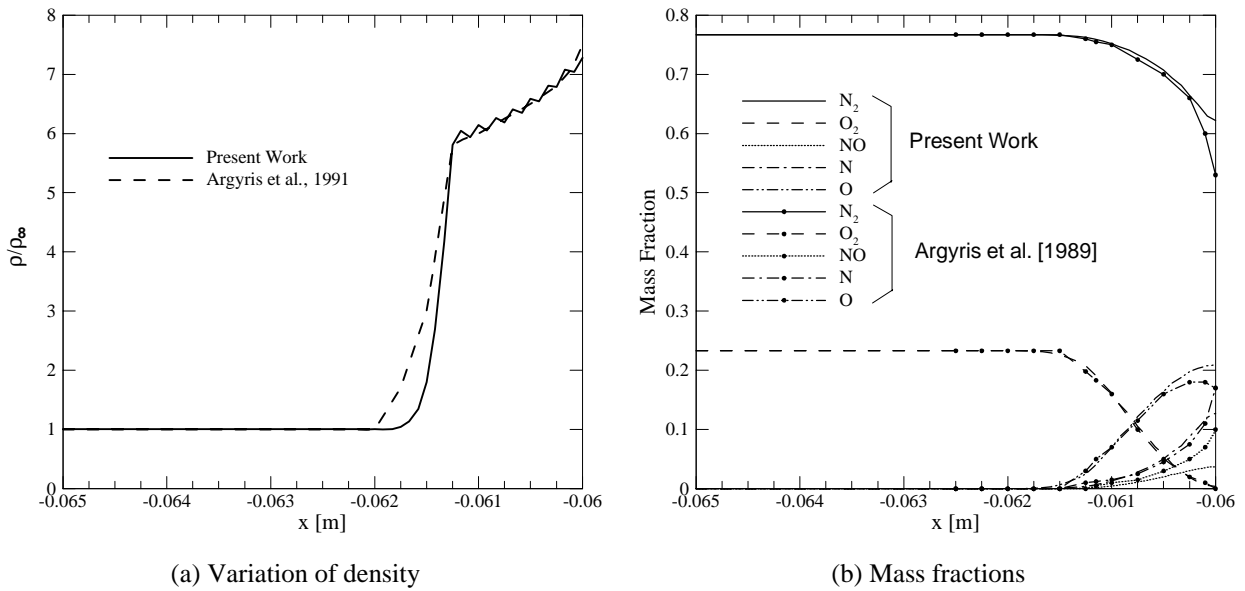


Figure 6. Variation of density (a) and mass fractions (b) along the stagnation line.

4.3 Hypersonic flow around the SARA vehicle

The non-diffusive hypersonic flow around the *Atmospheric Reentry Satellite* (SARA) is analyzed. Its geometry is constituted of a sphere-cone ensemble, as shown in Fig. (7).

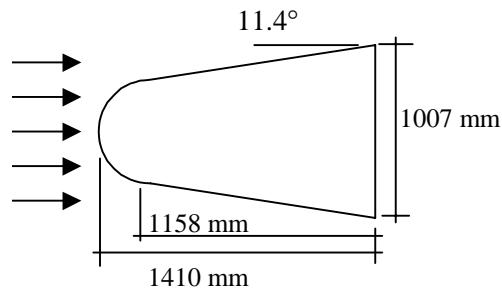


Figure 7. Geometry of the SARA vehicle.

The free-stream conditions are: Mach number = 12.7, velocity = 3570 m/s, temperature = 196 K, density = 1.6×10^{-3} kg/m³, pressure = 90.40 Pa, mass fraction of N₂ and O₂ are 0.767 and 0.233, respectively, mass fraction of the other species = 0.

To reduce the computational cost, only one fourth of the vehicle is analyzed. The finite element mesh is constituted of 44278 elements with 48303 nodes and is shown in Fig. (8a). In Fig. (8b) is shown the Mach number contours. In Fig. (9a) are shown the Mach number and translational and vibrational temperatures distributions along stagnation line, respectively. In Fig. (9b) are shown the mass fractions for the 5 species along stagnation line.

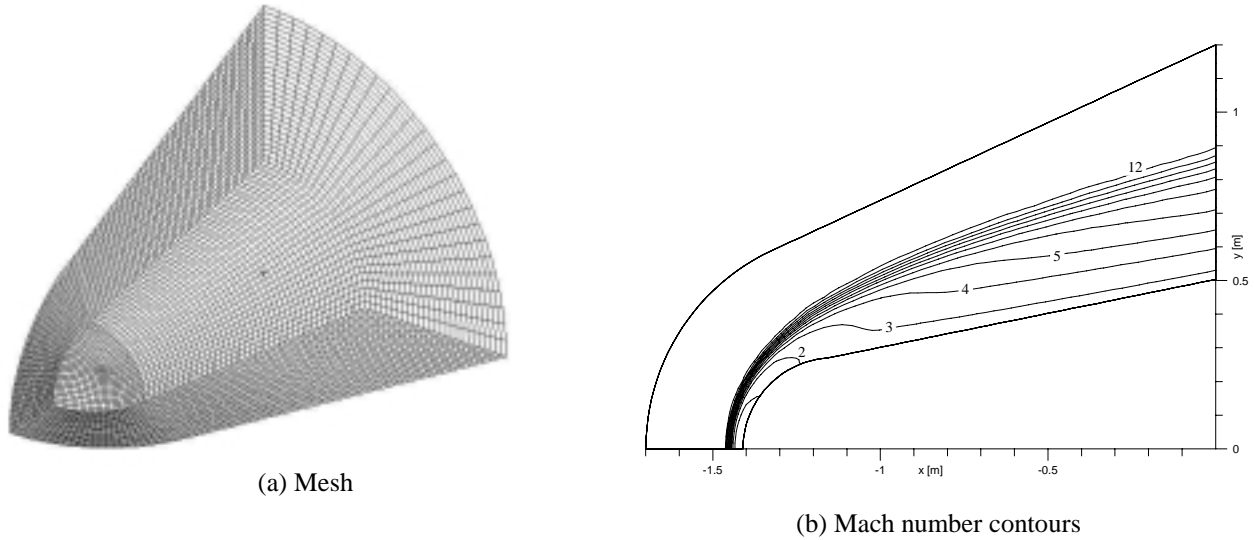


Figure 8. Finite element mesh (a) and Mach number contours (b).

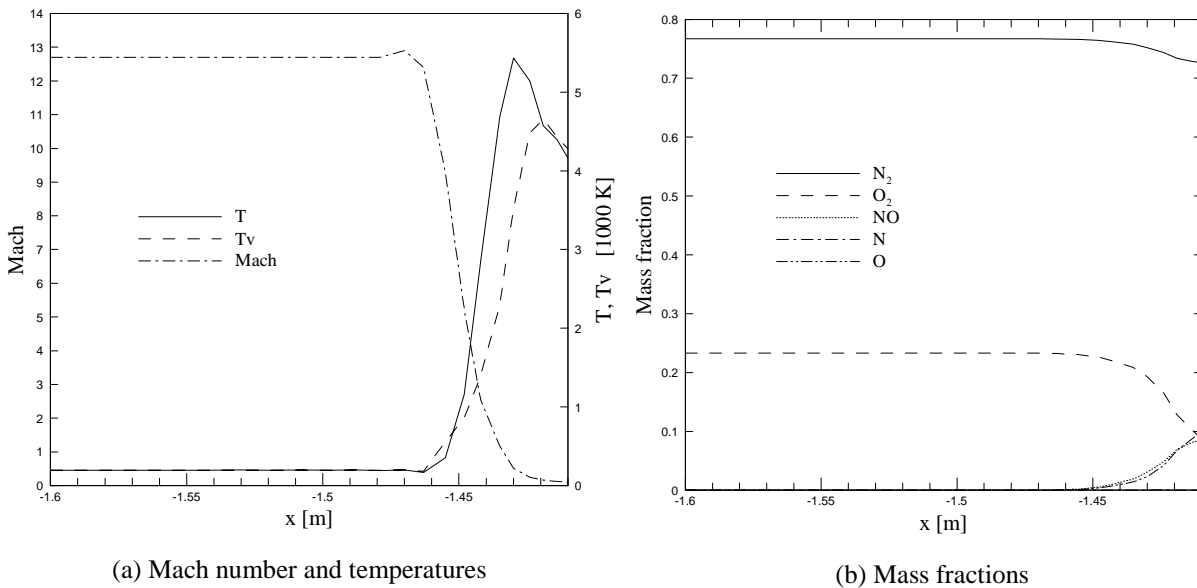


Figure 9. Mach number and temperatures (a) and mass fractions (b) along the stagnation line.

5. Conclusions

The numerical procedure proposed by the present work reproduces the experimental shock position for the nitrogen flow around a cylinder. In addition, the results obtained in the present work for the problem of hypersonic flow around a half-ellipse are in good agreement with those obtained numerically by Argyris *et al.* (1989, 1991). In all examples, the mass fractions of chemical species usually take more time to respond to the shock than the other properties (e.g. temperature). This phenomenon was expected since chemical reactions require a large number of collisions to occur, which demands certain amount of time. The vibrational temperature usually presents smaller values and respond a little later to the shock than the translational temperature. This was also expected since the molecules become vibrationally

excited only above a specific temperature (typically, 800 K for air at 1 atm.). Future works will include adaptive meshes as well as ionization processes.

6. Acknowledgements

The authors wish to thank the National Supercomputing Center of the Federal University of Rio Grande do Sul and the Brazilian Space Agency for their support.

7. References

- Ait-Ali-Yahia, D. & Habashi, W. G., 1997. "Finite Element Adaptive Method for Hypersonic Thermochemical Nonequilibrium Flows". *AIAA Journal*. Vol. 35, No. 8, pp. 1294-1302.
- Anderson, J. D., 1989. "Hypersonic and High Temperature Gas Dynamics". McGraw-Hill.
- Argyris, J., Doltsinis, I. S. & Friz, H. 1989. "Hermes Space Shuttle: Explorations of Reentry Aerodynamics". *Computer Methods in Applied Mechanics and Engineering*, Vol. 73, pp. 1-51.
- Argyris, J., Doltsinis, I. S. & Friz, H. 1990. "Studies on Computational Reentry Aerodynamics". *Computer Methods in Applied Mechanics and Engineering*, Vol. 81, pp. 257-289.
- Argyris, J., Doltsinis, I. S., Friz, H. & Urban., J. 1991. "An Exploration of Chemically Reacting Viscous Hypersonic Flow". *Computer Methods in Applied Mechanics and Engineering*, Vol. 89, pp. 85-128.
- Argyris, J., Doltsinis, I. S., Friz, H. & Urban., J. 1994. "Physical and Computational Aspects of Chemically Reacting Hypersonic Flows". *Computer Methods in Applied Mechanics and Engineering*, Vol. 111, pp. 1-35.
- Bird, R. B., Stewart, W. E. & Lightfoot, E. N. 1960. "Transport Phenomena". John Wiley & Sons.
- Brown, K. G. 1986. "Chemical and Thermal Nonequilibrium Heat-Transfer Analysis for Hypervelocity, Low Reynolds Number Flow", pages 445-477 of Moss, J. N. & Scott, C. D. (Editors), *Thermophysical Aspects of Re-Entry Flows*. Progress in Astronautics and Aeronautics. Vol. 103. AIAA.
- Codina, R. 1998. "Comparison of Some Finite Element Methods for Solving the Diffusion-Convection-Reaction Equation". *Computer Methods in Applied Mechanics and Engineering*. Vol. 156. pp. 185-210.
- Désidéri, J. A., 1991. "The Computation over Unstructured Grids of Inviscid Hypersonic Reactive Flow by Upwind Finite-Volume Schemes". Chapter 11, pages 387-446 of Murthy, T. K. S. (Editor). *Computational Methods in Hypersonic Aerodynamics*. Kluwer Academic Publishers.
- Donea, J. 1984. "A Taylor-Galerkin Method for Convective Transport Problems". *International Journal for Numerical Methods in Engineering*. Vol. 20. pp. 101-119.
- Gnoffo, P. A, Gupta, O. N. & Shinn, J. L., 1989. "Conservation Equations and Physical Models for Hypersonic Air Flows in Thermal and Chemical Nonequilibrium". NASA TP-2867.
- Hornung, H. G. 1972. "Non-equilibrium Dissociating Nitrogen Flow Over Spheres and Circular Cylinders". *Journal of Fluid Mechanics*. Vol. 53(1). pp. 149-176.
- Kessler, M. P., 2002. "Simulação Numérica de Escoamentos Hipersônicos em Não-Equilíbrio Termo-Químico através do Método dos Elementos Finitos". Ph.D. Thesis. Department of Mechanical Engineering. Federal University of Rio Grande do Sul. Porto Alegre. Brazil.
- Lax, P. & Wendroff, B. 1960. "Systems of Conservation Laws". *Comm. on Pure and Appl. Math*. Vol. 13. pp. 217-237.
- Lax, P. & Wendroff, B. 1962. "On the Stability of Difference Schemes". *Comm. on Pure and Appl. Math*. Vol. 15. pp. 363-371.
- Lax, P. & Wendroff, B. 1964. "Difference Schemes for Hyperbolic Equations with High Order Accuracy". *Comm. on Pure and Appl. Math*. Vol. 17. pp. 381-398.
- Lee, J. H. 1985. "Basic Governing Equations for the Flight Regimes of Aeroassisted Orbital Transfer Vehicles". pages 3-53 of Nelson, H. F. (Editor). *Thermal Design of Aeroassisted Orbital Transfer Vehicles*. Progress in Astronautics and Aeronautics. Vol. 96. AIAA.
- Men'shov, I. S. & Nakamura, Y., 2000. "Numerical Simulations and Experimental Comparisons for High-Speed Nonequilibrium Air Flows". *Fluid Dynamic Research*. Vol. 27, pp. 305-334.
- Moretti, G. & Abbett, M., 1966. "A Time-Dependent Computational Method for Blunt Body Flows". *AIAA Journal*, vol. 4(12), pp. 2136-2141.
- Park, C. 1985. "Problems of Rate Chemistry in the Flight Regimes of Aeroassisted Orbital Transfer Vehicles". pages 511-537 of Nelson, H. F. (Editor). *Thermal Design of Aeroassisted Orbital Transfer Vehicles*. Progress in Astronautics and Aeronautics. Vol. 96. AIAA.
- Park, C., 1986. "Convergence of Computation of Chemical Reacting Flows", pages 478-513 of Moss, J. N. & Scott, C. D. (Editors), *Thermophysical Aspects of Re-Entry Flows*. Progress in Astron. and Aeron. Vol. 103. AIAA.
- Park, C., 1990. "Nonequilibrium Hypersonic Aerothermodynamics". John Wiley.
- Safjan, A. & Oden, J. T. 1995. "High-Order Taylor-Galerkin Methods for Linear Hyperbolic Systems". *Journal of Computational Physics*. Vol. 120. pp. 206-230.
- Yoon, K. T., Moon, S. Y., Garcia, S. A., Heard, G. W. & Chung. T. J. 1998. "Flowfield-dependent mixed explicit-implicit (FDMEI) methods for high and low speed and compressible and incompressible flows". *Computer Methods in Applied Mechanics and Engineering*. Vol. 151(1-2). pp. 141-219.